Published online 21 November 2012 *Nucleic Acids Research, 2013, Vol. 41, No. 2* ***855–868***
doi:10.1093/nar/gks1095

Phosphoinositide 3-kinase beta controls replication factor C assembly and function

Javier Redondo-Muñoz[1], María Josefa Rodríguez[2], Virginia Silió[1], Vicente Pérez-García[1], José María Valpuesta[2] and Ana C. Carrera[1,*]

[1]Department of Immunology and Oncology and [2]Department of Macromolecular Structures, Centro Nacional de Biotecnología (CNB-CSIC), Darwin 3, Campus de Cantoblanco, Madrid E-28049, Spain

Received June 22, 2012; Revised October 17, 2012; Accepted October 19, 2012

ABSTRACT

Genomic integrity is preserved by the action of protein complexes that control DNA homeostasis. These include the sliding clamps, trimeric protein rings that are arranged around DNA by clamp loaders. Replication factor C (RFC) is the clamp loader for proliferating cell nuclear antigen, which acts on DNA replication. Other processes that require mobile contact of proteins with DNA use alternative RFC complexes that exchange RFC1 for CTF18 or RAD17. Phosphoinositide 3-kinases (PI3K) are lipid kinases that generate 3-poly-phosphorylated-phosphoinositides at the plasma membrane following receptor stimulation. The two ubiquitous isoforms, PI3Kalpha and PI3Kbeta, have been extensively studied due to their involvement in cancer and nuclear PI3Kbeta has been found to regulate DNA replication and repair, processes controlled by molecular clamps. We studied here whether PI3Kbeta directly controls the process of molecular clamps loading. We show that PI3Kbeta associated with RFC1 and RFC1-like subunits. Only when in complex with PI3Kbeta, RFC1 bound to Ran GTPase and localized to the nucleus, suggesting that PI3Kbeta regulates RFC1 nuclear import. PI3Kbeta controlled not only RFC1– and RFC–RAD17 complexes, but also RFC–CTF18, in turn affecting CTF18-mediated chromatid cohesion. PI3Kbeta thus has a general function in genomic stability by controlling the localization and function of RFC complexes.

INTRODUCTION

DNA structure remodeling events occur during DNA replication, repair and chromatin cohesion. Failure of any of these processes can promote genomic instability, characteristic of age-associated diseases and of cancer cells (1,2). To prevent this, cells use various protein complexes including helicases, replicases, polymerases, clamps and clamp loaders, which recruit appropriate machinery to chromatin for DNA maintenance processes.

Ring-type polymerases (found in all organisms) are formed by three components: the DNA polymerase, a trimeric protein ring (called sliding clamp) and the clamp–loader complex. PCNA (proliferating cell nuclear antigen) is the first described sliding clamp in eukaryotes that acts as a mobile platform for the DNA polymerases δ and ε during DNA replication; it is arranged in its trimeric structure around DNA by the clamp loader RFC (replication factor C) (reviewed in 3–9).

RFC consists of five subunits, one large (RFC1) and four small (RFC2–5). All subunits share two structurally conserved domains that comprise an ATPase module of the AAA^+ family. The large subunit, RFC1, also has extended N- (NT) and C-terminal (CT) regions (10,11). The NT region includes a conserved PCNA-binding motif that targets RFC to replication factories (10). The RFC1 CT domain (CTD) is less well characterized, although mutation experiments and structural analyses point to a role for CTD in RFC complex assembly and stability (10,11). Three additional RFC-like complexes are critical for other cellular processes; in these, the RFC1 subunit is replaced by Elg1 (RFC–Egl1), RAD17 (RFC–RAD17) or CTF18 (RFC–CTF18) (4). RFC and RFC-like complexes act as platforms for sliding clamp arrangement around DNA; all RFC are able to load PCNA-containing complexes onto DNA, but they act in distinct complexes and cellular situations, resulting in the function of RFC–Egl1 in genome stability, RFC–RAD17 in DNA repair, and RFC–CTF18 in chromatid cohesion (4,12–14).

The class I phosphoinositide 3-kinases (PI3K) are lipid kinases that catalyse *in vivo* production of

*To whom correspondence should be addressed. Tel: +34 91 585 4846; Fax: +34 91 372 0493; Email: acarrera@cnb.csic.es

phosphatidylinositols (PI)(3,4,5)P_3 and PI(3,4)P_2 at the plasma membrane. The PI3K are heterodimeric proteins consisting of a p110 catalytic (p110α, p110β or p110δ) and a p85 regulatory subunit; p110γ is structurally similar, but associates to distinct regulatory subunits (15–17). Whereas p110δ and p110γ are more abundant in hematopoietic cells and control the immune response (17), the catalytic subunits p110α and p110β are expressed ubiquitously and control cell division and cancer (18). p110α and p110β isoforms have distinct subcellular localizations and different functions (19–22). The classical function of PI3K is the generation of poly-phosphoinositides at the cell membrane; this is the case for p110α, which is found mainly in the cytosol and regulates insulin action and cell cycle entry. p110β also exerts this action but is more abundant in the nucleus, associates with PCNA and RAD17, and participates in DNA replication and repair (22–24).

Here we studied whether p110β regulates DNA homeostasis by controlling molecular clamp loading onto chromatin. We show that p110β associates directly with RFC1-like subunits and is necessary for RFC complex formation and function. Indeed, p110β association with RFC1-like subunits was needed for RFC, RFC–RAD17 and RFC–CTF18 complex assembly and function. In addition to controlling DNA replication and repair, p110β-regulated chromatin cohesion, supporting a general function in higher eukaryotes for p110β in the regulation of sliding clamp binding to chromatin. One mechanism by which p110β mediates this action is by regulating RFC1 nuclear import.

MATERIALS AND METHODS

Cell lines, cell culture and plasmids

U2OS, NIH3T3 and 293T cell lines were maintained in Dulbecco's modified Eagle's medium (Gibco-BRL) supplemented with 10% fetal bovine serum, 2 mM glutamine, 10 mM HEPES, 100 IU/ml penicillin and 100 μg/ml streptomycin.

Untagged wild type (WT)-p110β was donated by B. Vanhaesebroeck (Barts Cancer Institute, Cancer Research UK, London, UK). pSG5-myc-K805R-hp110β, -p110α and -p110β have been described (22). pCDNA3-Flag-RFC1, -RFC4 and -CTF18 were a gift of T. Todo (Kyoto University, Japan). pCDNA3-PCNA was donated by M. C. Cardoso (Max-Delbrück-Centrum, Berlin, Germany), RAD9 by H. G. Wang (Moffitt Cancer Center and Research Institute, Tampa, FL), and Flag-Ran and Flag-Q69L-Ran were from R. Pulido (Centro de Investigación Príncipe Felipe de Valencia, Spain). pET28-His-importin (Imp)-β was from R. A. Cerione (Cornell University, Ithaca, NY). Myc-p110β-mutant 1, -mutant 2 and the Flag-RFC1-mutant were generated using QuikChange site-directed mutagenesis (Stratagene) with appropriate oligonucleotides. shRNA for murine PI3K, RFC1 and RFC4 subunits and control-scrambled shRNA were custom-made (Origene Technologies). siRNA for human PI3K subunits or scrambled siRNA were custom-made (Invitrogen).

Antibodies and reagents

Western blot (WB) and immunoprecipitation (IP) assays were probed with the following antibodies: anti-Myc tag (9B11), -p-Chk-1 (Ser345), -p110β (all from Cell Signaling), anti-histone from Upstate Biotechnology (Millipore), -CenpA (Abcam), and anti-Flag, -β-actin and -tubulin from Sigma-Aldrich. Anti-p110α was donated by A. Klippel (Merck, Boston, MA). Anti-RFC1, -RFC4, -RAD17, -CTF18, -SMC1, -RAD9 and -cyclin B were from Santa Cruz Biotechnology, anti-PCNA from BD Transduction Labs, anti-His mAb from Clontech, Alexa488- and Cy3-labeled secondary antibodies from Molecular Probes, HRP-conjugated secondary antibodies from Dako and ECL from GE Healthcare. Colcemid was from Gibco-BRL. PIK75 and TGX221 were previously described (22).

IF, WB, IP and glycerol gradient

WB and IP were as described (22). For immunofluorescence (IF), cells were plated on cover slips and fixed with 4% formaldehyde [10 min, room temperature (RT)], then permeabilized with 0.3% Triton X-100 in PBS staining buffer (10 min), incubated with blocking buffer (0.1% TX-100, 3% BSA in PBS; 30 min), followed by incubation with primary antibody (1 h, RT, with end-to-end rocking). Unbound antibody was removed by washing cells three times with blocking buffer, and cells were incubated with appropriate secondary antibody (1:500, 1 h, RT). Samples were washed three times with blocking buffer and incubated with Vectashield mounting medium (Vector Laboratories); DAPI was used to stain DNA. Images were captured on a confocal fluorescence microscope with an Olympus FluoView (Olympus).

For glycerol gradients, NIH3T3 cell lysates prepared as above were loaded on an 8 ml gradient of 15–35% glycerol in buffer H (25 mM Hepes, 0.1 mM EDTA, 15% glycerol, 1 mM dithiothreitol (DTT), 1 mM PMSF) containing 0.1 M NaCl and centrifuged (234 100*g* in a SW41 rotor (Beckman Coulter), 20 h at 4°C. Fractions (0.5 ml) were collected from the top and proteins analysed by WB. Standard sedimentation markers were loaded in parallel glycerol gradients to determine sedimentation position (25).

In vitro transcription/translation

cDNAs were transcribed and translated in *vitro* in the presence of ^{35}S methionine using the TNT T7-coupled reticulocyte lysate system (Promega). In other experiments, Flag-RFC1 was transcribed and translated with Flag-Ran. *In vitro* binding of proteins was analysed by IP of Flag or Myc tags, or with anti-RFC1 or -Ran Ab, SDS-PAGE and autoradiography.

Transfection, subcellular fractionation and Ran pulldown assay

Cells were transfected with Lipofectamine Plus (Qbiogene) and cultured 48 h prior to analysis. For siRNA transfection, we used Lipofectamine Max (Qbiogene). For subcellular fractionation, cells were cultured for indicated

times/conditions and collected. Cytoplasmic, nuclear and chromatin fractions were isolated as described (26). Buffer A (10 mM Hepes pH 7.9, 10 mM KCl, 1.5 mM $MgCl_2$, 0.34 M sucrose, 10% glycerol, 1 mM DTT) was used for cytoplasmic extraction. Non-salt buffer for nuclear extraction was 3 mM EDTA, 0.2 mM EGTA and 1 mM DTT; for chromatin, samples were boiled and sonicated in Laemmli buffer and proteins extracted. In all cases, samples were quantified by BCA protein assay (Pierce) and same amount of protein analysed in WB. For DNA damage experiments, we transfected cells with different shRNAs. Cells were γ-irradiated (MARK 1) using a ^{137}Cs probe, collected after 24 h and analysed in WB.

For Ran pulldown assays, His6-Imp-β was expressed in *Escherichia coli*. For the assay, NIH3T3 cells were lysed and His6-Imp-β added to lysates (30 min, RT). The lysates with His6-Imp-β-bound proteins were incubated with Ni-chelating agarose beads (ABT; 1 h, 4°C, with rocking). The beads were pelleted, washed three times with lysis buffer plus 100 mM imidazole to eliminate background binding of non-specific proteins, and then resuspended in 5x Laemmli buffer for analysis by SDS-PAGE and WB.

Cell cycle

Cell cycle distribution was examined by DNA staining with propidium iodide and analysed by flow cytometry in a Cytomics FC500 (Beckman-Coulter). Cells were synchronized at G0/G1 by serum deprivation (19 h). After washing, cells were released by serum addition and analysed at indicated times. For mitosis, cells were synchronized by colcemid treatment (16 h), then cultured in complete medium (1 h) and fixed for IF, or enriched in mitotic cells by shaking off the culture disk. For S phase progression, cells were incubated with 10 μM BrdU (90 min), washed twice in fresh medium and harvested at indicated times using trypsin-EDTA. Cells were fixed in ice-cold 80% methanol (overnight, −20°C). Cells were resuspended in 2 N HCl with 0.5% Triton X-100 and pepsin (60 min, 37°C), washed twice with PBS, incubated with anti-BrdU-FITC (1 h, 37°C), washed again, and incubated with propidium iodide (30 min) and analysed by flow cytometry.

Electron microscopy

293T cells were transfected with Flag-RFC1 alone or with p110β siRNA. For immunogold labeling assays, cells cultured on coverslips (48 h) were fixed *in situ* with 4% paraformaldehyde (1 h, RT), permeabilized with PBS + 0.1% saponin (20 min) and blocked in a mixture of 2% BSA, 1% goat serum and 0.1% saponin in PBS (20 min). Primary antibody incubation with anti-Flag (60 min) was followed by incubation with goat-anti-mouse IgG-Nanogold (1:40, 60 min; Nanoprobes). Cells were fixed with 2.5% glutaraldehyde in PBS (60 min), washed with distilled water and silver-enhanced with HQ Silver (Nanoprobes), then stained with uranyl acetate, dehydrated in ethanol and embedded in epoxy resin (Fluka). Infiltrated samples were polymerized (60°C, 2 days). After polymerization, resin-containing cells were separated from the coverslip by dipping into liquid nitrogen. Ultrathin sections (70 nm) were cut in parallel to the monolayer, transferred to formvar-coated EM-buttonhole grids and stained with aqueous uranyl acetate and lead citrate. Images were captured on a Jeol JEM 1200 operating at 100Kv.

Sequence structure alignments

Models of the RFC complex were derived using the RFC crystal structure (PDB code: 1SXJ). p110β models were designed from our previous molecular model (27) and the published crystal structure (PDB code: 2Y3A). Potential sequences involved in p110β-RFC1 interaction were determined by BLAST search sequences in the NCBI PDB database. We analysed residues conserved among species in RFC1 and RFC1-like proteins. Similar sequences in p110α, p110β and other DNA-related proteins were proposed as RFC1-binding regions and candidate residues in RFC1 and p110β were screened in computational models of RFC and p85β/p110β complexes.

Statistical analyses

Statistical analyses were performed using StatView 512+. Fluorescence intensity was quantitated with ImageJ software. Statistical significance was evaluated with Student's *t*-test and the chi-square test calculated using Prism5 V.5.0 software. Error bars represent standard deviations of the mean values.

RESULTS

Purified p110β associates directly to RFC1

p110β knockdown reduces the binding of PCNA and of RAD9 to chromatin during DNA replication and repair (23,24). Since PCNA and RAD9 are sliding clamps, we sought to determine whether p110β affected molecular clamp loading onto chromatin. We studied whether p110β binds directly to molecular clamps or to clamp loaders.

To examine the association between p110 and these purified RFC subunits *in vitro*, we performed *in vitro* transcription/translation of the two ubiquitous PI3K subunits (p110α and p110β), and of RFC1, RFC4 and the RFC1-like protein CTF18. Both p110α and p110β (whose amino acid sequences are 42% identical) bound RFC1 and CTF18 *in vitro* (Figure 1A). Translation efficiency of the RFC4 + p110 reaction was similar to that of RFC1 + p110, near 1:1 (Figure 1A, left). Although IP of p110 was able to pulldown an amount of RFC1 similar to that of p110, it apparently failed to pulldown RFC4, which was undetectable when p110 was clearly visible (Figure 1A, right), suggesting inefficient p110 association with RFC4 (Figure 1A). Quantitation of the RFC1 or the CTF18 signal in complex with p110 showed significant association levels (nearly 1:1; Figure 1A). Reciprocal Flag-RFC IP assays detected p110α and p110β in complex with RFC1 and CTF18, but not with RFC4 (Figure 1B). Purified p110α and p110β interacted with

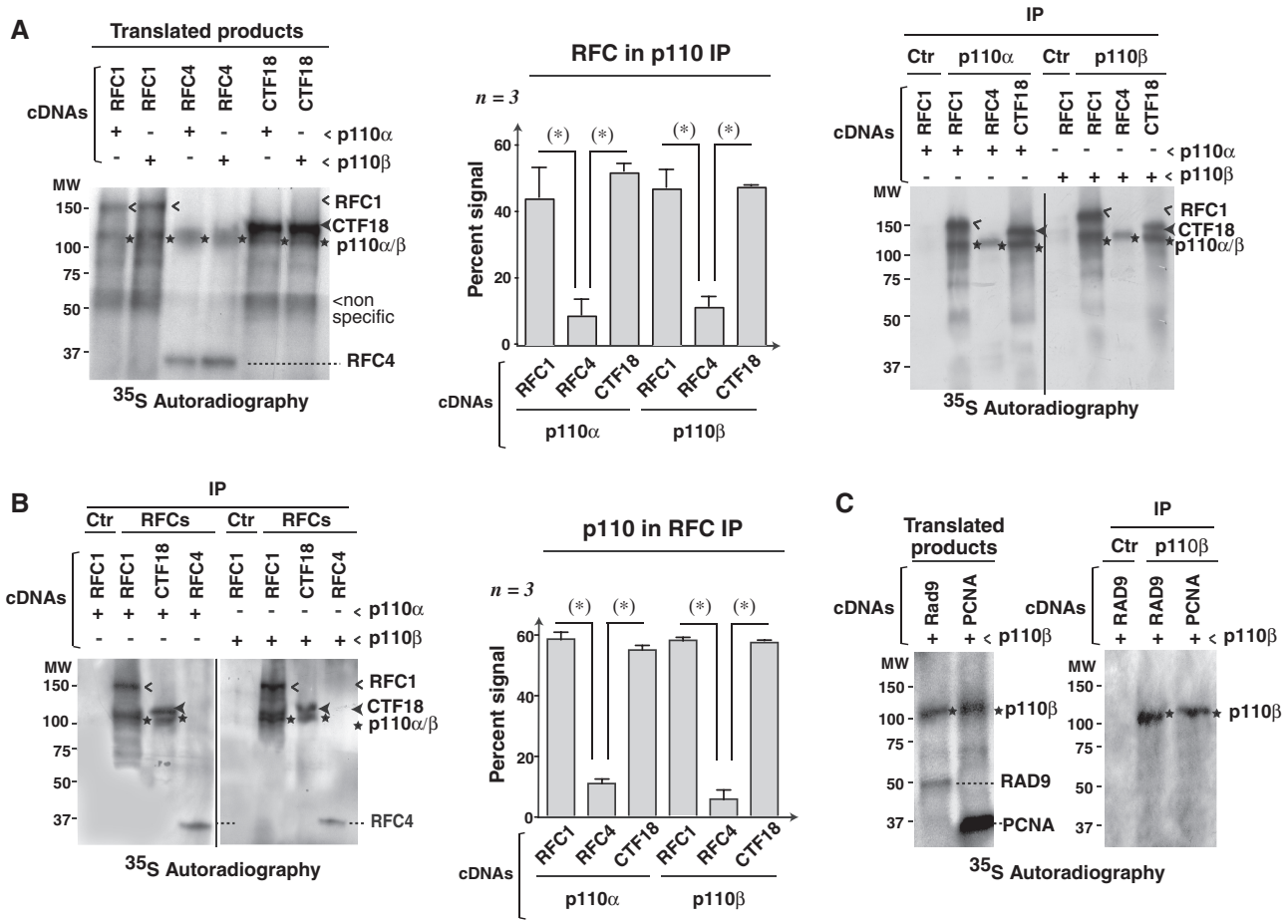

Figure 1. Purified p110α and p110β interact with RFC1 and CTF18. (**A**) cDNAs encoding myc-p110α or -p110β in combination with Flag-RFC1, -RFC4 or -CTF18 were transcribed/translated *in vitro* in the presence of ^{35}S-Met. Transcribed/translated products and IP myc-tagged proteins were analysed by SDS-PAGE and autoradiography. The graph shows RFC subunit signal intensity relative to total signal in p110 IP (100%); mean ± SEM ($n = 3$). (**B**) cDNAs encoding myc-p110α or -p110β in combination with Flag-RFC1, -RFC4 or -CTF18 were transcribed/translated *in vitro* and IP using anti-Flag Ab; IP and graph as in (A). (**C**) cDNA encoding myc-p110β was transcribed/translated with PCNA or RAD9. Resolved reaction products and IP proteins using anti-myc Ab were analysed by autoradiography. Stars indicate p110, empty arrowheads RFC-1, arrowheads CTF18, dashed lines RFC4, RAD9 and PCNA. * Student's *t*-test $P < 0.05$.

RFC1 in the absence of the PI3K p85 regulatory subunit, indicating that p110 subunits themselves associate to RFC1-like components.

p110β can also be isolated from cell extracts in complex with the molecular clamps PCNA and RAD9 (23,24); we tested whether p110β also associates directly to purified PCNA or RAD9, as above. p110β did not bind directly to PCNA or RAD9 (Figure 1C). Purified p110α and p110β thus associated *in vitro* to the clamp loader components RFC1 and CTF18, but not directly to the molecular clamps PCNA and RAD9.

p110β controls RFC complex assembly and localization

To assess whether p110 interacts with RFC1-like subunits *in vivo*, we analysed the association of endogenous proteins in an immortal murine fibroblast cell line (NIH3T3), and confirmed the results in a human tumor cell line (U2OS). Both cell lines expressed RFC1 and RFC4 normally, and expression was unaffected by p110α or p110β knockdown with interfering RNA (Supplementary Figure S1A). IP of RFC1 from U2OS or NIH3T3 cell lysates showed that p110β, but not p110α, associated to RFC1 *in vivo* (Figure 2A). Conversely, anti-p110β antibodies (Ab), but not anti-p110α Ab precipitated RFC1 (Figure 2A). Although purified p110β did not associate directly with RFC4 (Figure 1A and B), we detected co-precipitation of RFC4 with p110β in cell extracts (Figure 2A), since RFC1 and RFC4 both form part of the RFC complex. These results show that p110β, but not p110α, interacts with the RFC *in vivo*. We verified the status of native RFC1/p110β complexes by glycerol gradient sedimentation. In total extracts (not shown) and in nuclear extracts of U2OS cells, p110β was detected in fractions in which RFC1 and RFC4 were present (Figure 2B), validating the integrity of RFC1/p110β complexes.

Since p110β associated directly to RFC1, to determine whether p110β deletion affects RFC complex assembly, we depleted NIH3T3 cells of p110β using a specific shRNA. IP of RFC1 and detection of associated RFC4 in WB indicated that p110β depletion impaired RFC1/RFC4 association, and in turn PCNA binding to chromatin (Figure 2C). The reciprocal assay (RFC4 IP and

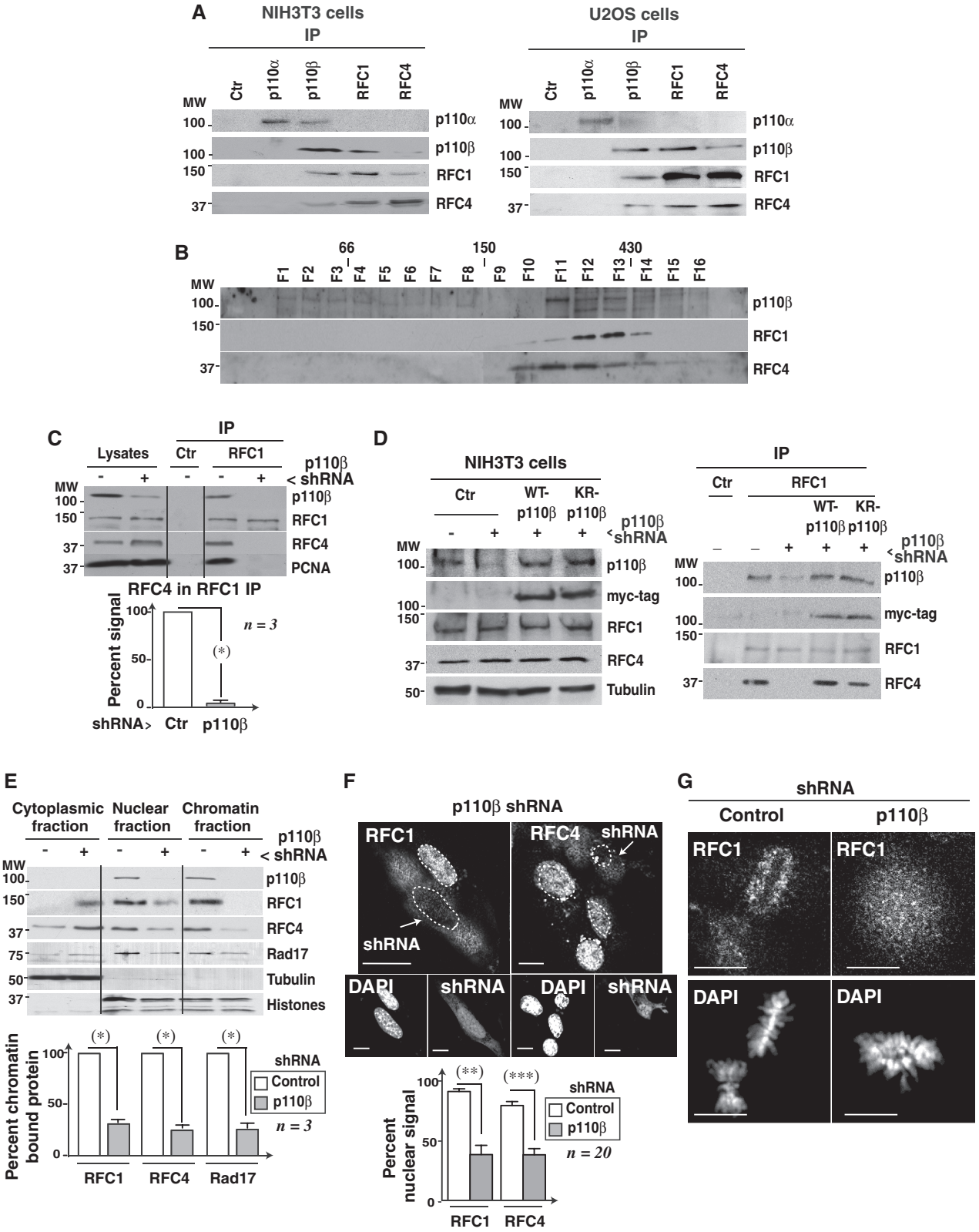

Figure 2. p110β but not p110α associates with RFC1 *in vivo* and controls RFC assembly. (**A**) NIH3T3 and U2OS cells were lysed and endogenous RFC1 or RFC4 association with p110α or p110β analysed by IP/WB using appropriate Ab. Representative assay of three with similar results. (**B**) NIH3T3 cell lysates were resolved in a 15–35% glycerol gradient; 0.5 ml fractions were collected from the top and proteins analysed by WB. (**C**) NIH3T3 cells were transfected with p110β shRNA (48 h); RFC1/RFC4 and RFC1/PCNA interactions were tested by IP/WB. The graph shows RFC4 signal intensity in RFC1 IP relative to maximal signal (in controls, 100%; mean ± SEM, $n = 3$). (**D**) NIH3T3 cells were depleted of endogenous p110β; after reconstitution with WT or KR-p110β, we examined RFC1 complex formation as in (C). (**E**) NIH3T3 cells transfected as in (C) were fractionated into cytoplasmic, nuclear and chromatin extracts and fractions analysed in WB. Tubulin and histones were used as

(continued)

detection of associated RFC1) confirmed that p110β silencing abrogated RFC complex formation, determined as RFC1/RFC4 association in NIH3T3 or U2OS cells (Supplementary Figure S1B). In contrast, p110α depletion did not affect RFC complex formation *in vivo* (Supplementary Figure S1C).

We previously showed that p110β control of DNA replication is largely kinase-independent (23). To test whether p110β interaction with RFC1 requires kinase activity, we depleted NIH3T3 cells of p110β and analysed RFC1 and p110β association after re-expression of WT or kinase inactive p110β (K805R-p110β) (23). RFC1 association with Myc-tagged-WT- or the KR-p110β mutant was similar, although slightly less efficient with KR-p110β (Figure 2D). Cell treatment with a selective inhibitor of p110β (23) only moderately reduced RFC1/p110β association (Supplementary Figure S1D). These data suggest that kinase activity is not essential for RFC1/p110β interaction.

RFC anchorage to chromatin requires correct RFC complex assembly (6); we hypothesized that since p110β depletion impairs complex formation, it would reduce RFC localization on DNA. We used fractionation analysis to study the influence of p110β expression on RFC localization; NIH3T3 cells transfected with p110β shRNA were separated into cytoplasmic, nuclear and chromatin fractions. p110β silencing reduced nuclear and chromatin-bound RFC1 and RFC4, and also reduced binding of the RFC1-like subunit Rad17 to chromatin (Figure 2E).

We tested whether the reduction in nuclear and chromatin-bound RFC1 and RFC4 in p110β-depleted NIH3T3 cells was also detectable by IF. RFC1 and RFC4 are mainly nuclear (28). Transfection with p110β shRNA led to diffuse cytoplasmic staining of RFC1 and a decreased nuclear signal for RFC4 (Figure 2F). During mitosis in control cells, RFC1 and RFC4 localized in the vicinity of chromosomes, and p110β silencing reduced the concentration of RFC1 surrounding chromosomes (Figure 2G). These data confirm the functional link of p110β with RFC1 *in vivo*, and indicate that p110β expression is needed for correct RFC complex assembly and localization.

RFC deletion affects DNA replication and repair similarly to p110β knockdown

p110β is essential for S phase progression and DNA repair, as is regulates correct binding of the molecular clamps PCNA and RAD9 to chromatin (23,24). To study whether p110β affects DNA replication and repair by impairing RFC complex formation, we tested whether RFC4 or p110β knockdown affected these responses similarly. To analyse correct induction of the cell response to DNA damage, we examined activation of the checkpoint protein kinase 1 [Chk1, (29)]. After γ-irradiation of NIH3T3 cells, phospho-Chk1 levels were reduced both in p110β- and in RFC4-depleted cells compared to controls (Figure 3A).

To compare p110β and RFC function in DNA replication, we monitored expression of cyclin B, a mitotic cyclin whose levels are increased throughout S phase (30). We reduced p110β or RFC4 expression with shRNA in cell cycle-synchronized NIH3T3 cells. Both treatments downregulated cyclin B levels during S phase (Figure 3B), reduced PCNA binding to chromatin (Figure 3C), and altered S phase progression in transfected cells (Figure 3D). Comparison of cell cycle profiles in asynchronous cultures, however, showed that RFC4 depletion (like that of p110β) (23) induced a slight increase in S phase cell proportion that might result from a delayed S phase entry and a prolonged S phase duration due to reduced velocity of DNA replication (23) (Figure 3D). Interference with RFC complex formation by depletion of one of its subunits (RFC4) thus induced defects in DNA repair, replication and cell cycle progression that were also observed after p110β deletion.

p110β is necessary for RFC-like complex function

We found that p110β depletion abrogates RFC1/RFC4 complex formation, PCNA association with RFC1 and PCNA/RFC binding to chromatin (Figures 2B and 3C). To determine whether p110β has a general function in mediating RFC complex formation, we reduced p110β expression levels and analysed RFC–RAD17 association after DNA damage as well as RFC–CTF18 complex formation in mitosis. NIH3T3 cells were transfected with p110β-specific shRNA (48 h) and γ-irradiated, after which we confirmed reduction of p110β levels in lysates (Figure 4A). In controls, Rad17 bound to RFC4 after irradiation; however, p110β depletion reduced Rad17/RFC4 interaction and in turn, Rad17 association with Rad9 (Figure 4A). To study RFC–CTF18 complex dependence on p110β expression, U2OS cells were transfected with p110α or p110β siRNA and mitotic cells enriched by colcemid treatment or culture plate shake-off (mitotic cells are less adherent to the substrate). We confirmed that p110α or p110β silencing reduced the expression of their targets, but not that of CTF18, RFC4 or SMC1 (Figure 4B). Depletion of p110β, but not of p110α, decreased CTF18/RFC4 association (Figure 4B and Supplementary Figure S1E).

RFC–CTF18 is a weak PCNA loader that controls the velocity of replication fork and chromatid cohesion (12,14,31–33). To test whether p110β deletion affects RFC–CTF18 function, we analysed chromatid cohesion. One consequence of reducing sister chromatid cohesion is an increase in the inter-kinetochore (KT) distance in metaphase (34). Bipolar chromosome capture by microtubules

Figure 2. Continued
cytoplasmic and nuclear/chromatin controls. The graph shows RFC signal intensity in the chromatin of p110β knocked-down cells relative to that of controls (100%). (**F**) NIH3T3 cells transfected with GFP plus p110β or control shRNA (48 h) were analysed by IF using RFC Ab; DNA was stained with DAPI. Arrows indicate GFP-transfected cells (see insets). Nuclei are indicated with a dashed line. The graph shows nuclear RFC signal intensity relative to total signal (100%). Mean ± SEM, $n = 20$. (**G**) NIH3T3 cells transfected as in (F) (24 h) were colcemid treated (16 h), released in medium (1 h) and analysed as in (F). Bars = 10 μm. * Student's *t*-test $P < 0.05$; ** $P < 0.01$; *** $P < 0.001$. See Supplementary Figure S1.

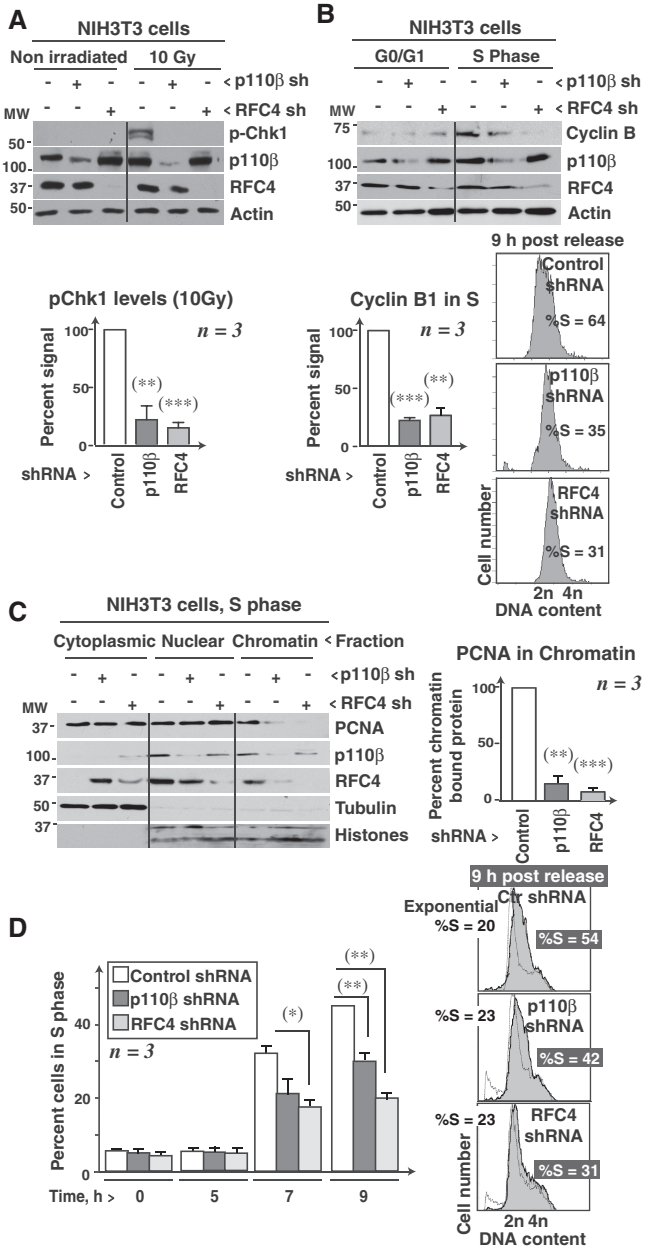

Figure 3. Downregulation of RFC or p110β alters S phase progression and Chk1 activation. (**A**) NIH3T3 cells were transfected with control, p110β or RFC4 shRNA (24 h), cells were irradiated (10 Gy) or untreated, and cultured for 24 h. Phospho-Chk1 and protein expression were analysed in WB. The graph shows p-Chk1 signal intensity relative to the p-Chk1 signal in controls (100%, mean ± SEM, $n = 3$). (**B**) Unirradiated NIH3T3 cells were transfected as in (A). After 24 h, cells were rendered quiescent by serum deprivation (19 h) and released by serum addition until S phase (9 h, FACS profiles shown). Cyclin B expression was analysed in WB and quantitated as in (A). Mean ± SEM ($n = 3$). (**C**) Unirradiated NIH3T3 cells were treated as in (B). After 9 h serum treatment, cells were fractionated and analysed in WB. Quantitation was as in (A); mean ± SEM ($n = 3$). (**D**) Unirradiated NIH3T3 cells treated as in (B) were serum-released for different times. The graph shows the percentage of S phase cells at different times (mean ± SEM; $n = 3$). Images show representative profiles of exponential growth or synchronized S phase entry (9 h post-release). * Student's *t*-test $P < 0.05$; ** $P < 0.01$; *** $P < 0.001$.

also increases this distance moderately, although to a lesser extent than cohesion defects (34). Nonetheless, to exclude potential bipolar attachment differences, we compared the cells in metaphase when all chromatid pairs show bipolar attachment. We transfected U2OS cells with control, p110α or p110β siRNA, synchronized them with colcemid (16 h), released them in medium (1 h), and measured the inter-KT distance in metaphase cells. Only p110β-depleted cells, but not control or p110α-depleted cells showed increased inter-KT distance (Figure 4C).

The mechanism that controls establishment of cohesion is not fully understood, particularly in mammals, but SMC1, SMC3, SCC1, SCC3 cohesins as well as ESCO2 (yeast Ctf7/Eco1), Wap1 and Pds5a are known to be necessary for chromatid cohesion (32,33). RFC–CTF18 controls progression of the replication fork along cohesin-associated DNA, as well as cohesin binding and, in turn, cohesion (4,32). To confirm cohesion regulation by p110β, we examined whether p110β silencing affected the binding to DNA of one of the essential cohesins, SMC1. In control and p110α siRNA-transfected cells, CTF18 and SMC1 were found in the chromatin fraction; in contrast, in p110β-depleted cells, SMC1 and CTF18 levels in chromatin were markedly reduced (Figure 4D). These data show that p110β also affects RFC–CTF18 complex formation and cohesion, supporting a general role for p110β in RFC complex assembly and function.

A conserved Lys/Asp motif in RFC1 is involved in the p110β interaction

RAD17 and CTF18 are RFC1 homologs (4). After sequence alignment of RFC1, RAD17 and CTF18, we sought conserved sequences that might explain their binding to p110β. We identified two potential conserved regions that aligned in the three clamp loader subunits; the first was in the AAA^+ ATPase domain (residues 647–658) and the second at the RFC-1 C terminus (residues 836–845). The residues in the AAA^+ domain are exposed in the inner region of the RFC/PCNA structure (5) and correspond to the ATPase P-loop that is part of the ATP-binding site (35). We thus focused on the second region encompasing RFC1 residues $Lys^{841}Asp^{842}$ (KD region; Figure 5A). This region is conserved from yeast to mammals and is exposed at the RFC/PCNA surface (Supplementary Figure S2A and B) permitting protein–protein interactions. RFC has several conserved domains; the AAA^+ module is composed of RFC domains 1 and 2, located before RFC domain 3 (5). The KD motif (yeast KN) is located in an exposed alpha helix at the end of the RFC conserved domain 2 [(5), Supplementary Figure S2C].

We replaced the KD residues with non-polar residues to generate the KD-RFC1 mutant (Figure 5A). To compare p110β association with WT or mutant RFC1, we performed *in vitro* transcription/translation and used autoradiography to visualize RFC1 in complex with immunoprecipitated p110β. Quantification of autoradiographs showed that p110β associated significantly greater with WT RFC1 than with the KD-RFC1 mutant (Figure 5B). To determine whether the KD mutation

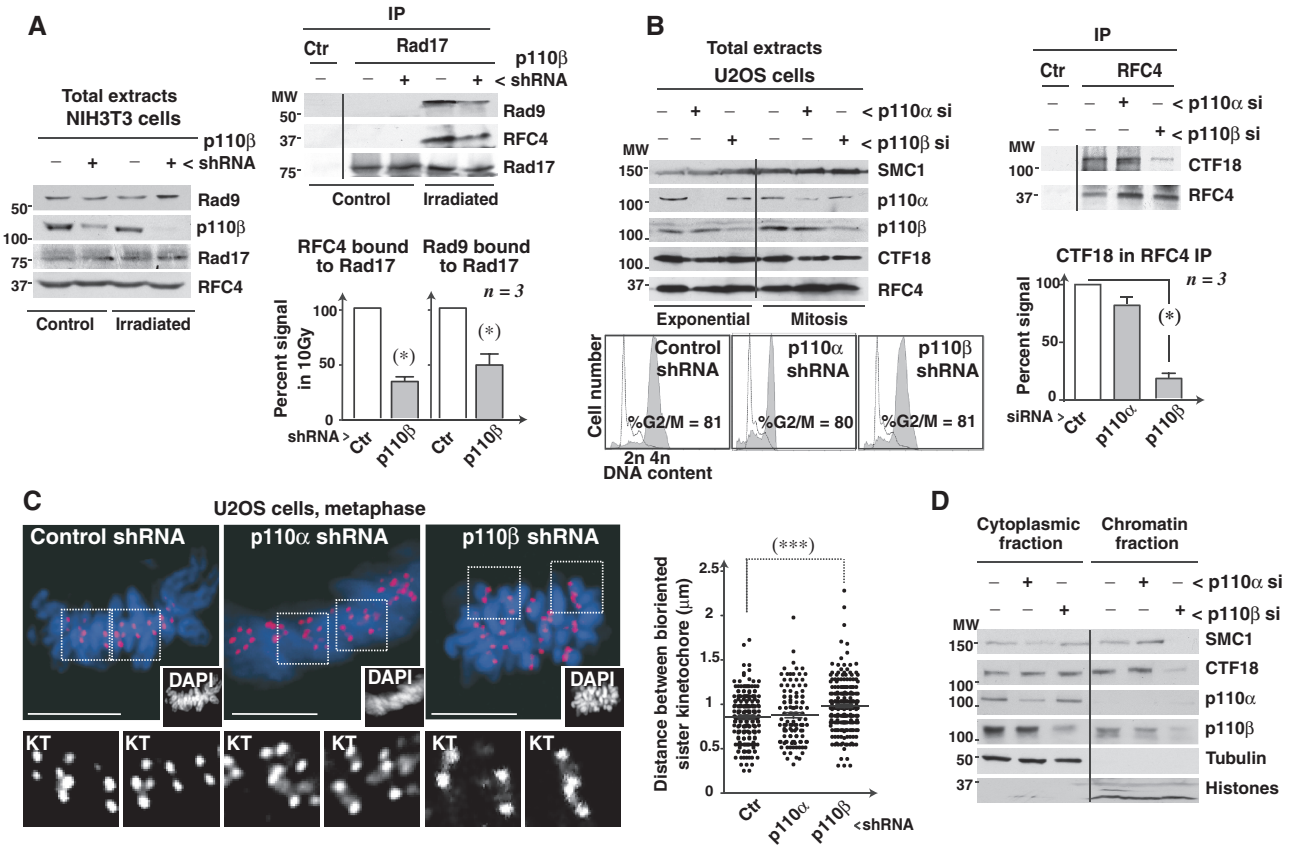

Figure 4. p110β silencing reduces RFC–CTF18 complex assembly and function. (**A**) NIH3T3 cells were transfected with control or p110β-specific shRNA (24 h), cells were irradiated (10 Gy) or left untreated, and cultured for 24 h before lysis. Protein expression in lysates was analysed by WB; Rad17/RFC4 association was analysed by IP/WB. The graph shows RFC4 or Rad9 signal intensity in Rad17 IP relative to maximal signal (RFC4 or Rad9 signal in Rad17 IP in controls, 100%; mean ± SEM, $n = 3$). (**B**) U2OS cells were transfected with indicated siRNA (24 h); cells were maintained in exponential growth or colcemid-synchronized (16 h), released in medium (1 h) and lysed. Protein expression in lysates was analysed by WB. Endogenous CTF18 association with RFC4 was analysed by IP/WB using appropriate Ab. FACS profiles show cell cycle distribution after colcemid treatment. (**C**) U2OS cells treated as in (B) were examined by IF using CenpA Ab to visualize KTs; DNA was stained with DAPI. The graph shows the distance (μm) between sister KT (mean ± SEM). Each dot represents a single KT; $n = 20$ cells. (**D**) U2OS cells treated as in (B) were fractionated into cytoplasmic and chromatin extracts, and these analysed in WB. Tubulin and histones were used as controls. * Student's t-test $P < 0.05$; *** $P < 0.001$.

affected only RFC1/p110β interaction, or also the RFC1/RFC4 intersubunit interaction, we tested KD-RFC1 mutant binding to RFC4 *in vitro* (Figure 5C). Purified WT RFC1 and KD-RFC1 associated to RFC4 at similar levels (Figure 5C), ruling out an effect of this region on RFC1/RFC4 intersubunit interactions. These findings show that RFC1 binding to p110β is mediated by the conserved KD residues. Localization of the KD homolog residues in the *Saccharomyces cerevisae* RFC crystal structure shows that they are proximal to the CTD domain (Supplementary Figure S2C and D), which regulates RFC complex assembly (10).

We also tested the effect of *in vivo* KD-RFC1 expression. We transfected NIH3T3 cells with WT RFC1 or the KD mutant and studied complex formation. KD mutation impaired RFC1/p110β association *in vivo* (Figure 5D). Moreover, although *in vitro* association of the purified KD-RFC1 mutant with RFC4 was similar to that of WT RFC1 (Figure 5C), *in vivo* since RFC complex formation (examined as RFC1 binding to RFC4) requires RFC1 association to p110β, we detected a lower interaction of RFC4 with KD-RFC1 (compared with RFC1), leading to significantly lower RFC complex formation (Figure 5D). These results confirm the idea that the conserved KD residues in RFC1 mediate association with p110β *in vivo*. Parallel to the reduction in RFC1/p110β association in KD-RFC1 mutant-expressing cells, we detected an increase in cytosolic KD-RFC1 (Figure 5E), indicating that RFC1/p110β association affects RFC1 intracellular localization.

A p110 CT region is necessary for interaction with RFC1

Both p110α and p110β bind to RFC1 *in vitro,* suggesting that the region involved in p110 association with RFC1 is common to both p110 subunits. The RFC1 KD residues, which mediate its association with p110, are polar and exposed; to determine the p110β region that mediates RFC1 association, we aligned p110α and p110β sequences and searched for conserved, polar and exposed residues that could establish this interaction. We pinpointed two regions in p110α and p110β with exposed polar residues that are

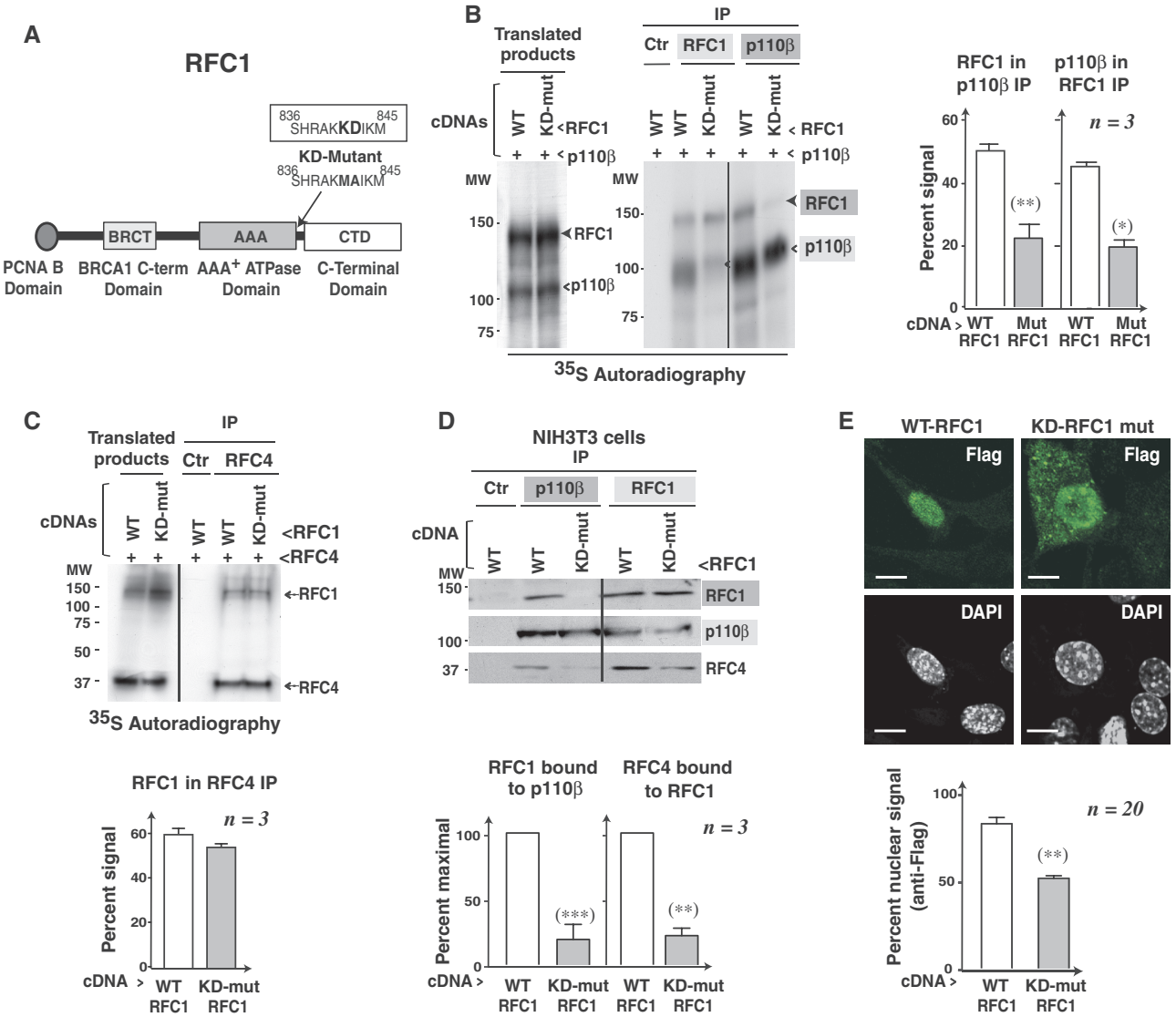

Figure 5. A conserved Lys/Asp motif in RFC1 is involved in its interaction with p110β. (**A**) RFC1 domain structure and potential sequence involved in interaction with p110β. The KD residues shared by RFC1, RAD17 and CTF18 were replaced in RFC1 with non-polar residues to generate the RFC1 mutant. (**B**) cDNA encoding myc-p110β was transcribed and translated with WT Flag-RFC1 or Flag-KD-RFC1 mutant. Translated products (left) and IP using anti-myc or -Flag Ab (right) were resolved by SDS-PAGE. The graphs show RFC1 signal in p110β IP or that of p110β in RFC1 IP compared to maximal signal (in controls; 100%). Mean ± SEM ($n = 3$). (**C**) Flag-RFC1-WT or Flag-RFC1-mutant were transcribed/translated in combination with Flag-RFC4, and RFC complex formation was determined in RFC4 IP. The graph shows RFC1/RFC4 association relative to maximal signal (in controls; 100%). Mean ± SEM ($n = 3$). (**D**) NIH3T3 cells transfected with WT Flag-RFC1 or KD-RFC1 mutant (48 h) were lysed and immunoprecipitated using anti-p110β or -Flag Ab. Graphs as in (B); mean ± SEM ($n = 3$). (**E**) NIH3T3 cells were transfected as in (D) and analysed by IF using anti-Flag Ab; DNA was stained with DAPI. The graph shows RFC1 signal intensity in the nucleus relative to total cell signal (100%). Mean ± SEM ($n = 20$ cells). Bars = 10 μm. * Student's t-test $P < 0.05$; ** $P < 0.01$; *** $P < 0.001$. See Supplementary Figure S2.

conserved across species (Figure 6A). The first, with a motif similar to that found in helicases, is located upstream of the p110 Ras-binding domain (residues 141–150), whereas the other, found in the p110 catalytic C terminus (residues 1031–1038) has a motif found in topoisomerase, RAD50, Cdc45 and bromodomain-containing proteins (Figure 6A). In each of these regions, we replaced polar with non-polar residues to generate two p110β mutants (Figure 6A). We synthesized WT RFC1, p110β and the p110β mutants, and tested association of the purified products by IP and autoradiography. p110β and p110β-mutant 1 associated efficiently with RFC1; in contrast, p110β-mutant 2 showed significantly less association (Figure 6B). In NIH3T3 cells transfected with WT or mutant p110β, we found reduced p110β-mutant 2 association with RFC1 (Figure 6C).

To analyse whether, as a result of impaired RFC1/p110β complex formation, replication was impaired in NIH3T3 cells expressing KD-RFC1 or p110β-mutant 2, we depleted endogenous RFC1 and reconstituted expression using shRNA-resistant WT or KD-RFC1, or alternatively, we knocked-down p110β and reconstituted cells with WT or p110β-mutant 2. We compared S phase progression by BrdU pulse-chase, which permits

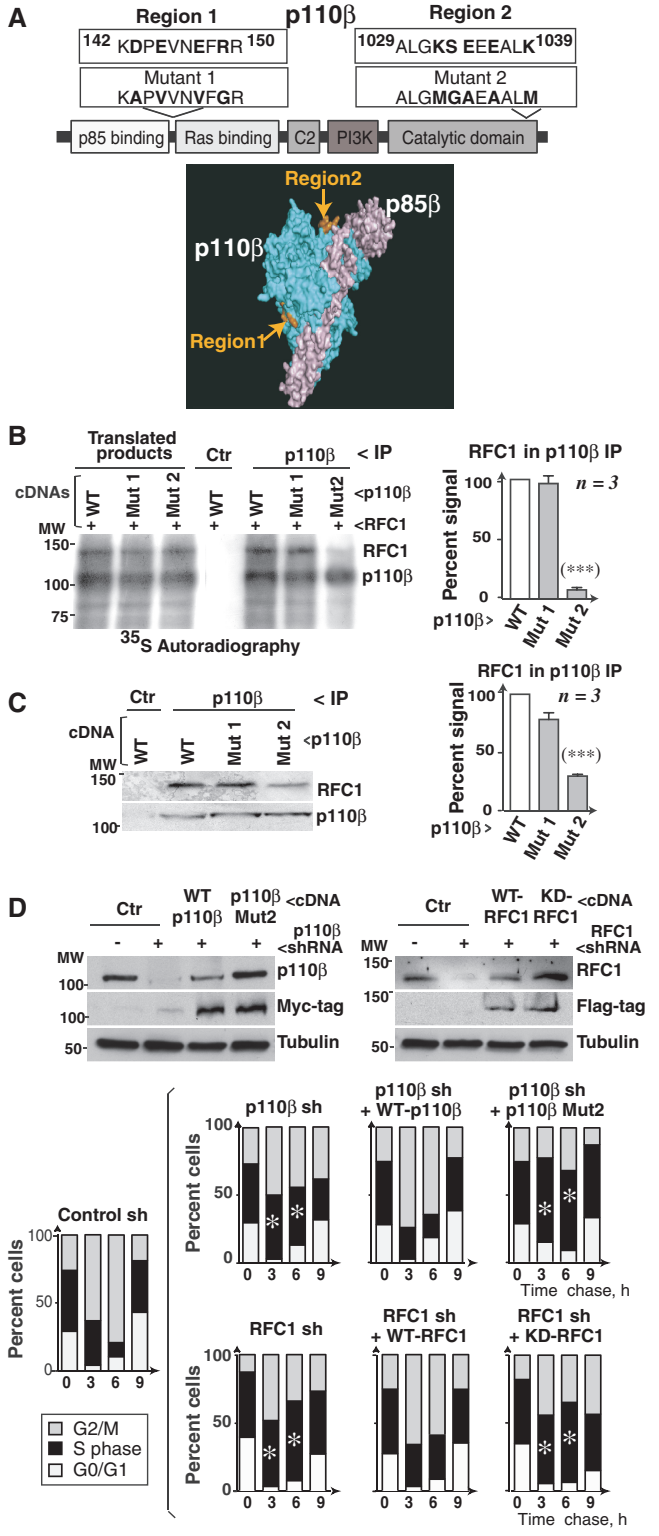

Figure 6. RFC1 binds to a CT motif in p110β. (**A**) Structure of the p85β (pink)/p110β (blue) complex. Regions 1 and 2 are polar, exposed, conserved regions (in p110α and p110β) potentially involved in RFC/p110β interaction. Amino acid sequence of p110β mutants 1 and 2. (**B**) cDNA encoding Flag-RFC1 was transcribed/translated in combination with myc-p110β-WT, -mutant 1 or -mutant 2 in the presence of ^{35}S-Met. Translated products (left) or IP prepared using anti-myc Ab (right) were resolved in SDS-PAGE. The graph shows the RFC1 signal in p110β IP relative to maximal signal (RFC1 signal in complex with p110β-WT; 100%). Mean ± SEM ($n = 3$). (**C**) NIH3T3 cells were transfected with the p110β forms (48 h); p110β proteins and IP from extracts prepared using anti-Myc Ab were tested in WB. The graph shows RFC1 signal in p110β IP relative to maximum (as in B). Mean ± SEM ($n = 3$). (**D**) NIH3T3 cells were depleted of endogenous p110β or of RFC1 using shRNA, and reconstituted by transfection with cDNA encoding WT or KR-p110β, or WT or RFC1-KD, respectively. Protein expression was analysed in WB (top). The DNA replication rate was measured by BrdU incorporation (90 min) in cells collected at different times after resuspension in fresh medium. Bar graphs show the percentage of cells in each cell cycle phase. White asterisks indicate statistically significant distribution differences compared to control shRNA cells. Mean ± SEM ($n = 3$). * Student's *t*-test $P < 0.05$; *** $P < 0.001$.

measurement of the DNA replication rate (23). The results confirmed defective replication speed in RFC1- or p110β-depleted cells, the correction mediated by reconstitution with WT RFC1 or p110β, and the replication defect of cells expressing RFC1-KD or p110β mutant 2 (Figure 6D). The results show that p110β CT residues 1031–1038 regulate its association with RFC1.

p110β deletion reduces RFC1–Ran interaction and affects RFC1 nuclear localization

Cytoplasmic retention correlates with defects in RFC function, since nuclear localization is necessary for RFC complex formation and function (36,37). RFC1, RAD17 and CTF18 have nuclear localization signals (NLSs) that mediate their Ran-GTPase-dependent nuclear localization (37). Since p110β silencing impaired RFC complex formation and function as well as RFC1 nuclear localization (Figure 2), we postulated that p110β association with RFC1 subunits modulates RFC1 nuclear import.

We analysed whether RFC1 associates directly with Ran-GTPase, by performing *in vitro* transcription/translation followed by autoradiography to test for Ran binding to RFC1. In the absence of other proteins, purified RFC1 associated to Ran (Figure 7A). Direct RFC1 association to Ran was not anticipated, as Ran association is normally Imp mediated; in cytoplasm, NLS-containing proteins bind to Imp-α and -β and are transported to the nucleus, where Imp-β binds Ran-GTP to release the NLS protein (38,39). To determine whether Ran also associates with RFC1 *in vivo*, we immunoprecipitated RFC1 from NIH3T3 cells and tested its association with Ran in WB. The results showed *in vivo* RFC1 association with Ran (Figure 7B).

We studied the effect of p110β silencing on the RFC1/Ran interaction *in vivo*. In control and p110α siRNA-transfected U2OS cells, RFC1 associated with Ran; in contrast, RFC1 association to Ran was markedly reduced in p110β-depleted U2OS or NIH3T3 cells (Figure 7C), showing that p110β expression is necessary for RFC1 interaction with Ran. p110β also has a functional NLS (27). In cells, Ran could bind RFC1 indirectly, through p110β. In our hands, however, purified p110β alone or with p85β did not appear to associate directly with Ran (Figure 7D) excluding that RFC1 binding to Ran reflects an indirect interaction *via* p110β. Our findings show that purified RFC1 associates directly

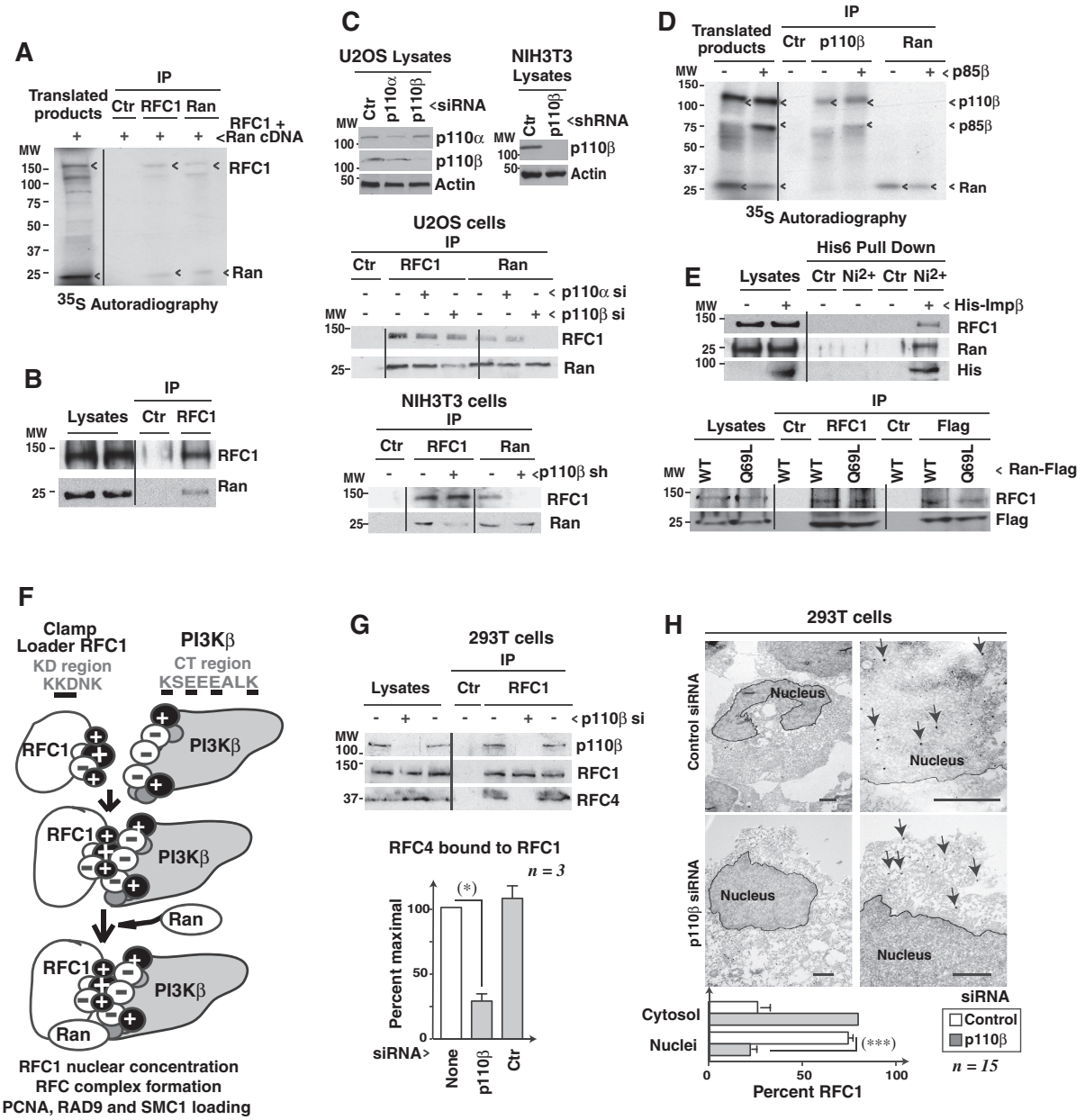

Figure 7. p110β expression is necessary for RFC1 association with Ran. (**A**) cDNAs encoding Flag-RFC1 and Flag-Ran were transcribed/translated *in vitro*. Translated products and IP (Ab indicated) were resolved by SDS-PAGE. (**B**) NIH3T3 cells were lysed and endogenous RFC1/p110β interaction examined by IP of RFC1 and WB. (**C**) NIH3T3 or U2OS cells were transfected with indicated shRNA or siRNA (48 h). Cells were lysed and RFC1/Ran interactions were tested by IP/WB using appropriate Ab. (**D**) cDNAs encoding myc-p110β and Flag-Ran (± HA-p85β) were synthesized *in vitro*. Translated products were analysed as in (A). (**E**) NIH3T3 cell extracts (top) were incubated with His-Imp-β beads and pulled down proteins were analysed in WB. NIH3T3 cells were also transfected with WT or Q69L-Ran (48 h) (bottom). Extracts were immunoprecipitated and analysed in WB as indicated. (**F**) Scheme of p110β action on RFC1. (**G**) 293T cells were transfected with Flag-RFC1-WT and p110β siRNA (48 h). RFC complex formation was analysed by IP/WB. The graph shows RFC4 signal intensity in RFC1 IP relative to maximal (in controls, 100%; mean ± SEM, $n = 3$). (**H**) 293T cells were transfected as in (G). RFC1 localization was determined using anti-Flag Ab and secondary Ab fused to nanogold particles. Bars = 1000 nm. The graph shows the percentage of RFC1 particles in the nucleus or cytosol. * Student's *t*-test $P < 0.05$ (F) and Fisher's exact test (G) $P < 0.001$.

with Ran-GTPase *in vitro*, but in cells, this interaction requires p110β expression, suggesting that only RFC1/p110β complexes bind to Ran.

To evaluate whether RFC1 binds to active or inactive forms of Ran *in vivo*, we took advantage of the ability of Imp-β to bind Ran-GTP and used it as bait to pulldown Ran-GTP. Imp-β pulled down RFC1, suggesting that RFC1 binds to active Ran (Figure 7E, top). As an alternative approach, we transfected cells with Flag-WT Ran or with the active Flag-Q69L-Ran mutant (40), and

examined the complexes by IP of Ran or of RFC1 and detection of associated proteins in WB. Both WT and active Ran bound similarly to RFC1 (Figure 7E) suggesting that RFC1 might bind active and inactive Ran. Our findings show that although RFC1 associates directly with Ran-GTPase *in vitro*, this interaction requires p110β expression in cells, suggesting that only when it is in complex with p110β, RFC1 adopts a conformation and/or localization that allows RFC1/Ran interaction. RFC1 association with Ran might regulate its nuclear entry, and in turn RFC1 association with other RFC subunits and effective chromatin binding by molecular clamps (model in Figure 7F).

To confirm the contribution of p110β to RFC1 nuclear localization, we assessed Flag-RFC1 localization in control or p110β siRNA-transfected 293T cells by transmission electron microscopy (TEM). We first confirmed that p110β silencing impairs RFC1/RFC4 association in these cells (Figure 7G). TEM using a Flag primary antibody showed that whereas in control cells RFC1 localized to the nucleus, in p110β siRNA-transfected cells, a large percentage of the electron-opaque particles corresponding to RFC1 were excluded from the nucleus (Figure 7H).

DISCUSSION

The assembly of homo- or heterotrimeric clamps in a ring shape around DNA is a complex, ATP-consuming process assisted by clamp loaders; RFC and RFC-like complexes support this process. RFC complexes are formed by five small subunits (RFC2–5) and a large RFC1 or RFC1-like subunit. Here we show that a p110β CT binds to a conserved Lys-Asp motif present in RFC1 and the RFC1-like subunits RAD17 and CTF18. This association is necessary for RFC–RFC1, RFC–RAD17 and RFC–CTF18 complex formation, as p110β depletion results in defective assembly of all these complexes, in deficient sliding clamp loading onto chromatin, and in defective sliding clamp-mediated cell responses. Indeed, interference with RFC complex formation either by p110β or by RFC4 silencing yielded similar DNA replication and repair defects. In addition, p110β−regulated RFC–CTF18 mediated chromatid cohesion. We show that p110β acts on RFC by regulating RFC1 association with Ran-GTPase, resulting in RFC1 nuclear localization.

We show that a conserved RFC1 Lys-Asp (KD) motif mediates association with p110β. Conserved Lys in RFC subunits are proposed to mediate interaction with DNA; however, these lysines are all located in the first domain (domain 1) of the AAA+ module (5) (Supplementary Figure S2C). The KD motif involved in p110β association is located in an exposed alpha helix at the end of the AAA^{+} module (domain 2) (5), just before another conserved region in RFC subunits (domain 3, Supplementary Figure S2C). Although the crystallized fragment of *S. cerevisae* RFC1 (RFCA) lacks the extended unique NT domain and most of the CTD, a small CTD region is present in the crystal and is found in proximity to the Lys-Asn peptide (corresponding to the KD motif in mammals) (Supplementary Figure S2D). Although the primary action of p110β is to facilitate RFC nuclear import, it is possible that p110β interaction with the RFC1 KD motif affects CTD structure, and in turn RFC complex assembly (10). Since p110β binds to chromatin (27), it might also regulate RFC binding to DNA.

RFC complexes are components of conserved DNA molecular machines; there are four known RFC complexes (RFC–RFC1, RFC–CTF18, RFC–RAD17 and RFC–ELG1). Although all RFC are able to load PCNA onto chromatin, they have different requirements, bind to different proteins and result in distinct RFC functions in DNA homeostasis (4,12–14). Both p110α and p110β bound to RFC1 *in vitro,* suggesting that the region involved in p110 association with RFC1 is present in both p110 subunits. The RFC1 KD residues, which mediate its association with p110, are polar and exposed. We aligned p110α and p110β sequences and searched for polar, exposed residues that could mediate p110 interaction with RFC1, and identified two candidate sequences. Mutation of one of these (the ALGKSEE EALK motif at the CT end of p110) abrogated interaction with RFC1. Three-dimensional structural analysis of the p85β/p110β heterodimer shows that in p110β (alpha helix 11), this region forms part of the p110β regulatory square that encompasses alpha helices 10, 11 and 12, as well as the activation and catalytic loops (41). The p85β nSH2 and cSH2 domains contact this regulatory square, maintaining p110β in an inactive conformation (41). The binding of p85β and RFC1 to the same region could explain why p110β associates to RFC1 without p85β, since p85β and RFC1 might compete for binding to this region. RFC1/p110β interaction near the regulatory square might affect p110β activity; future studies will address this possibility. The polar nature of the regions involved in RFC1/p110β association supports the likelihood of a strong, apparently 1:1 electrostatic interaction (Figure 1) between these molecules (Figure 7).

To define the first event controlled by p110β in the RFC cycle, we focused on the observation that p110β silencing reduced the nuclear localization of RFC1. Given the molecular function of RFC complexes, appropriate nuclear translocation of their subunits is crucial for their correct assembly and function (36). Indeed, an interaction between RFC4 and RIα regulates RFC4 nuclear localization; disruption of this interaction alters cell proliferation (28). RFC1, RAD17, CTF18 and p110β localize to the nucleus (27,37). RFC-1 and RFC1-like subunits have two conserved NLS sequences that might mediate nuclear import of these proteins (37). Nonetheless, in the canonical nuclear import mechanism, NLS-containing proteins bind to Imps that mediate nuclear import. Once in the nucleus, Imp-β binding to Ran-GTP mediates release of NLS-containing proteins from the Imps (38,39). We found that purified RFC1, but not p110β, binds directly to Ran, suggesting that RFC1 might use an alternative mechanism or combination of mechanisms for its nuclear import, as described for other proteins (39,42). We show that although RFC1 associates with Ran *in vitro*, RFC1/Ran interaction (and RFC1 nuclear localization) requires p110β expression in cells. p110β depletion not only reduced RFC1 nuclear localization in interphase; even in mitosis, p110β silencing reduced the

RFC1 concentration near chromosomes (Figure 2G). As Ran regulates protein proximity to chromosomes (43), defective RFC1/Ran association after p110β silencing might also impair RFC1 translocation to DNA. Although open questions remain, our results suggest that the regulation of RFC1 nuclear localization is a primary event by which p110β controls correct RFC complex function.

The other ubiquitous PI3K isoform, p110α, interacted with RFC1 *in vitro*, although no association was observed *in vivo*. These findings concur with the primarily cytosolic localization and function of p110α, which controls receptor-induced plasma membrane phosphoinositide production; p110β also binds to membrane receptors and regulates phosphoinositide production, but a large fraction of p110β localizes in the nucleus and is able to bind DNA (22,23,27).

Our observations support a general function for p110β in the control of distinct RFC complexes. We show that p110β deletion induced a phenotype similar to that of RFC4 deletion in S phase progression and DNA repair checkpoint activation. Based on the role of of p110β in RFC–CTF18 complex formation, we postulate that cell functions controlled by this RFC would also be affected by p110β deletion. RFC–CTF18 regulates elongation as well as cohesion of sister chromatids (33). Although the mechanism that controls the establishment of cohesion is not fully understood (33,44), it seems clear that the RFC–CTF18 complex regulates cohesion, at least in yeast (12,31,32). We show that the inter-KT distance in mammalian cell metaphase is markedly higher in p110β-depleted cells than in controls, an indication of defective cohesion; a similar phenotype is found in cells depleted of SMC1, one of the critical cohesins (34). We also examined SMC1 binding to chromatin, which was reduced after p110β silencing. These results indicate that p110β-depleted cells have defective chromatid cohesion.

Sliding clamp proteins girdle DNA and act as mobile platforms for organizing DNA processes. Aberrations in DNA stability and maintenance are associated with oncogenesis and age-related diseases (1). The study of the molecular mechanisms that control DNA metabolism and the proteins involved will yield new targets for prevention and therapy for these diseases. Our observations support the conclusion that p110β has a general function in control of RFC/RFC-like complex functions, thereby protecting genomic stability.

SUPPLEMENTARY DATA

Supplementary Data are available at NAR Online: Supplementary Figures 1 and 2.

ACKNOWLEDGEMENTS

The authors thank Drs B. Vanhaesebroeck for the p110β plasmid, T. Todo for the RFC1, RFC4 and CTF18 plasmids, M. C. Cardoso for PCNA, H. G. Wang for RAD9 plasmids, R. Pulido for Ran and A. Klippel for anti-p110α Ab; the authors also thank C. Mark for editorial assistance.

FUNDING

Spanish Ministry of Science and Innovation (MICINN; Juan de la Cierva postdoctoral fellowship to J.R.M.); Spanish Association Against Cancer (AECC); MICINN [SAF2010-21019, BFU2010-15703/BMC and the Network of Cooperative Research in Cancer RD07/0020/2020]; Madrid regional government [S-BIO-0189/06]; and Sandra Ibarra Foundation. Funding for open access charge: [SAF2010-21019].

Conflict of interest statement. None declared.

REFERENCES

1. Branzei,D. and Foiani,M. (2010) Maintaining genome stability at the replication fork. *Nat. Rev. Mol. Cell Biol.*, **11**, 208–219.
2. Broderick,S., Rehmet,K., Concannon,C. and Nasheuer,H.P. (2010) Eukaryotic single-stranded DNA binding proteins: central factors in genome stability. *Subcell. Biochem.*, **50**, 143–163.
3. Bruck,I. and O'Donell,M. (2001) The ring-type polymerase sliding clamp family. *Genome Biol.*, **2**, 3001.1-3.
4. Majka,J. and Burgers,P.M. (2004) The PCNA-RFC families of DNA clamps and clamp loaders. *Prog. Nucleic Acid Res. Mol. Biol.*, **78**, 227–260.
5. Bowman,G.D., O'Donnell,M. and Kuriyan,J. (2004) Structural analysis of a eukaryotic sliding DNA clamp-clamp loader complex. *Nature*, **429**, 724–730.
6. Indiani,C. and O'Donnell,M. (2006) The replication clamp-loading machine at work in the three domains of life. *Nat. Rev. Mol. Cell Biol.*, **7**, 751–761.
7. Lopez de Saro,F.J. (2009) Regulation of interactions with sliding clamps during DNA replication and repair. *Curr. Genom.*, **10**, 206–215.
8. Patel,S.S., Pandey,M. and Nandakumar,D. (2011) Dynamic coupling between the motors of DNA replication: hexameric helicase, DNA polymerase, and primase. *Curr. Opin. Chem. Biol.*, **15**, 595–605.
9. Poveda,A.M., Le Clech,M. and Pasero,P. (2010) Transcription and replication: breaking the rules of the road causes genomic instability. *Transcription*, **1**, 99–102.
10. Uhlmann,F., Cai,J., Gibbs,E., O'Donnell,M. and Hurwitz,J. (1997) Deletion analysis of the large subunit p140 in human replication factor C reveals regions required for complex formation and replication activities. *J. Biol. Chem.*, **272**, 10058–10064.
11. Kim,J., Robertson,K., Mylonas,K.J., Gray,F.C., Charapitsa,I. and MacNeill,S.A. (2005) Contrasting effects of Elg1-RFC and CTF18-RFC inactivation in the absence of fully functional RFC in fission yeast. *Nucleic Acids Res.*, **33**, 4078–4089.
12. Hanna,J.S., Kroll,E.S., Lundblad,V. and Spencer,F.A. (2001) Saccharomyces cerevisiae CTF18 and CTF4 are required for Sister Chromatid Cohesion. *Mol. Cell. Biol.*, **21**, 3144–3158.
13. Zou,L., Cortez,D. and Elledge,S.J. (2002) Regulation of ATR substrate selection by Rad17-dependent loading of Rad9 complexes onto chromatin. *Genes Dev.*, **16**, 198–208.
14. Bermudez,V.P., Maniwa,Y., Tappin,I., Ozato,K., Yokomori,K. and Hurwitz,J. (2003) The alternative CTF18-Dcc1-CTF8-replication factor C complex required for sister chromatid cohesion loads proliferating cell nuclear antigen onto DNA. *Proc. Natl Acad. Sci. USA*, **100**, 10237–10242.
15. Hiles,I.D., Otsu,M., Volinia,S., Fry,M.J., Gout,I., Dhand,R., Panayotou,G., Ruiz-Larrea,F., Thompson,A., Totty,N.F. *et al.* (1992) Phosphatidylinositol 3-kinase: structure and expression of the 110 kd catalytic subunit. *Cell*, **70**, 419–429.
16. Hu,P., Mondino,A., Skolnik,E.Y. and Schlessinger,J. (1993) Cloning of a novel, ubiquitously expressed human phosphatidylinositol 3-kinase and identification of its binding site on p85. *Mol. Cell. Biol.*, **13**, 7677–7688.
17. Okkenhaug,K. and Fruman,D.A. (2010) PI3Ks in lymphocyte signaling and development. *Curr. Top. Microbiol. Immunol.*, **346**, 57–85.

18. Vogt,P.K., Hart,J.R., Gymnopoulos,M., Jiang,H., Kang,S., Bader,A.G., Zhao,L. and Denley,A. (2010) Phosphatidylinositol 3-kinase: the oncoprotein. *Curr. Top. Microbiol. Immunol.*, **347**, 79–104.
19. Bi,L., Okabe,I., Bernard,D.J. and Nussbaum,R.L. (2002) Early embryonic lethality in mice deficient in the p110beta catalytic subunit of PI 3-kinase. *Mamm. Genome*, **13**, 169–172.
20. Bi,L., Okabe,I., Bernard,D.J., Wynshaw-Boris,A. and Nussbaum,R.L. (1999) Proliferative defect and embryonic lethality in mice homozygous for a deletion in the p110alpha subunit of phosphoinositide 3-kinase. *J. Biol. Chem.*, **274**, 10963–10968.
21. Foukas,L.C., Claret,M., Pearce,W., Okkenhaug,K., Meek,S., Peskett,E., Sancho,S., Smith,A.J., Withers,D.J. and Vanhaesebroeck,B. (2006) Critical role for the p110alpha phosphoinositide-3-OH kinase in growth and metabolic regulation. *Nature*, **441**, 366–370.
22. Marques,M., Kumar,A., Cortes,I., Gonzalez-Garcia,A., Hernandez,C., Moreno-Ortiz,M.C. and Carrera,A.C. (2008) PI3K p110alpha and p110beta regulate cell cycle entry, exhibiting distinct activation kinetics in G1 phase. *Mol. Cell. Biol.*, **28**, 2803–2814.
23. Marques,M., Kumar,A., Poveda,A.M., Zuluaga,S., Hernandez,C., Jackson,S., Pasero,P. and Carrera,A.C. (2009) Specific function of phosphoinositide 3-kinase beta in the control of DNA replication. *Proc. Natl Acad. Sci. USA*, **106**, 7525–7530.
24. Kumar,A., Fernandez-Capetillo,O. and Carrera,A.C. (2010) Nuclear phosphoinositide 3-kinase beta controls double-strand break DNA repair. *Proc. Natl Acad. Sci. USA*, **107**, 7491–7496.
25. Murakami,T., Takano,R., Takeo,S., Taniguchi,R., Ogawa,K., Ohashi,E. and Tsurimoto,T. (2010) Stable interaction between the human proliferating cell nuclear antigen loader complex Ctf18-replication factor C (RFC) and DNA polymerase {epsilon} is mediated by the cohesion-specific subunits, Ctf18, Dcc1, and Ctf8. *J. Biol. Chem.*, **285**, 34608–34615.
26. Méndez,J. and Stillman,B. (2000) Chromatin association of human origin recognition complex, cdc6, and minichromosome maintenance proteins during the cell cycle: assembly of prereplication complexes in late mitosis. *Mol. Cell. Biol.*, **20**, 8602–8612.
27. Kumar,A., Redondo-Muñoz,J., Perez-Garcia,V., Cortes,I., Chagoyen,M. and Carrera,A.C. (2011) Nuclear but not cytosolic phosphoinositide 3-kinase beta has an essential function in cell survival. *Mol. Cell. Biol.*, **31**, 2122–2133.
28. Gupte,R.S., Pozarowski,P., Grabarek,J., Traganos,F. and Darzynkiewicz,Z. (2005) RIalpha influences cellular proliferation in cancer cells by transporting RFC40 into the nucleus. *Cancer Biol. Ther.*, **4**, 429–437.
29. Jackson,S.P. and Bartek,J. (2009) The DNA-damage response in human biology and disease. *Nature*, **461**, 1071–1078.
30. Katula,K.S., Wright,K.L., Paul,H., Surman,D.R., Nuckolls,F.J., Smith,J.W., Ting,J.P., Yates,J. and Cogswell,J.P. (1997) Cyclin-dependent kinase activation and S-phase induction of the cyclin B1 gene are linked through the CCAAT elements. *Cell Growth Differ.*, **8**, 811–820.
31. Mayer,M.L., Gygi,S.P., Aebersold,R. and Hieter,P. (2001) Identification of RFC (CTF18p, CTF8p, Dcc1p): an alternative RFC complex required for sister chromatid cohesion in S. cerevisiae. *Mol. Cell.*, **7**, 959–970.
32. Terret,M.E., Sherwood,R., Rahman,S., Qin,J. and Jallepalli,P.V. (2009) Cohesin acetylation speeds the replication fork. *Nature*, **462**, 231–234.
33. Skibbens,R.V. (2010) Buck the establishment: reinventing sister chromatid cohesion. *Trends Cell. Biol.*, **20**, 507–513.
34. Maresca,T.J. and Salmon,E.D. (2009) Intrakinetochore stretch is associated with changes in kinetochore phosphorylation and spindle assembly checkpoint activity. *J. Cell. Biol.*, **184**, 373–381.
35. Hanson,P.I. and Whiteheart,S.W. (2005) AAA+ proteins: have engine, will work. *Nat. Rev. Mol. Cell Biol.*, **6**, 519–529.
36. Gupte,R.S., Sampson,V., Traganos,F., Darzynkiewicz,Z. and Lee,M.Y. (2006) Cyclic AMP regulates the expression and nuclear translocation of RFC40 in MCF7 cells. *Exp. Cell. Res.*, **312**, 796–806.
37. Merkle,C.J., Karnitz,L.M., Henry-Sanchez,J.T. and Chen,J. (2003) Cloning and characterization of hCTF18, hCTF8, and hDCC1. *J. Biol. Chem.*, **278**, 30051–30056.
38. Strom,A.C. and Weis,K. (2001) Importin-beta-like nuclear transport receptors. *Genome Biol.*, **2**, REVIEWS3008 1–9.
39. Wagstaff,K.M. and Jans,D.A. (2009) Importins and beyond: non-conventional nuclear transport mechanisms. *Traffic*, **10**, 1188–1198.
40. Giri,D.K., Ali-Seyed,M., Li,L.Y., Lee,D.F., Ling,P., Bartholomeusz,G., Wang,S.C. and Hung,M.C. (2005) Endosomal transport of ErbB-2: mechanism for nuclear entry of the cellsurface receptor. *Mol. Cell. Biol.*, **25**, 11005–11018.
41. Zhang,X., Vadas,O., Perisic,O., Anderson,K.E., Clark,J., Hawkins,P.T., Stephens,L.R. and Williams,R.L. (2011) Structure of lipid kinase p110beta/p85beta elucidates an unusual SH2-domain-mediated inhibitory mechanism. *Mol. Cell*, **41**, 567–578.
42. Fagotto,F., Glück,U. and Gumbiner,B.M. (1998) Nuclear localization signal-independent and importin/karyopherin-independent nuclear import of beta-catenin. *Curr. Biol.*, **8**, 181–190.
43. Clarke,P.R. and Zhang,C. (2008) Spatial and temporal coordination of mitosis by RanGTPase. *Nat. Rev. Mol. Cell. Biol.*, **9**, 464–477.
44. Nasmyth,K. (2011) Cohesin: a catenase with separate entry and exit gates? *Nat. Cell Biol.*, **13**, 1170–1177.